Relative energies and electronic structures of CoO polymorphs through *ab initio* diffusion quantum Monte Carlo

Kayahan Saritas,* Jaron T. Krogel, and Fernando A. Reboredo†
Materials Science and Technology Division, Oak Ridge National Laboratory, Oak Ridge, Tennessee 37831, USA

(Received 9 July 2018; revised manuscript received 6 September 2018; published 16 October 2018)

We present a many-body diffusion quantum Monte Carlo (DMC) study on the ground- and excited state properties of crystalline CoO polymorphs. To our knowledge, DMC is the only electronic structure method available to provide correct energetic ordering within experimental error bars between the three CoO polymorphs: rocksalt, wurtzite, and zinc blende. We compare these results to density functional theory (DFT) using state-of-the-art functionals such as SCAN. For the structural properties, such as the lattice parameters and bulk moduli, our results are comparable to HSE and SCAN. Using DMC, we calculated the indirect and direct optical gaps as 3.8(2) and 5.2(2) eV. Our indirect optical gap compares well with the conductivity measurements of 3.6(5) eV and GW calculations with 3.4 eV. Similarly, we obtained the DMC indirect and direct quasiparticle gaps as 3.9(2) and 5.5(2) eV. DMC direct quasiparticle gaps compare well with the direct band gap of 5.53 eV obtained from ellipsometry studies.

DOI: 10.1103/PhysRevB.98.155130

I. INTRODUCTION

Cobalt (II) monoxide is a late transition metal oxide that exists in three polymorphic crystalline structures: slightly distorted rocksalt (RS), cubic zinc blende (ZB), and hexagonal wurtzite (WZ). RS phase is known to be the most stable phase, while ZB phase is the least stable [1–6]. In contrast to the experiments, *ab initio* theoretical modeling of these materials, with density functional theory (DFT), has met with mixed success [7–9]. Recently developed DFT functionals, such as SCAN [10,11], have improved the predictions on the ground and excited states of CoO [8]. Yet, to our knowledge, no DFT functional yields the qualitatively correct ordering between all CoO polymorphs. This polymorphism problem has also been observed in transition metal oxides such as MnO [12] and less dramatically in MgO and ZnO [13]. Accurate modeling of these polymorphs is of interest to a greater scientific and technical community, due to their implications in the stability of related complex materials [8,11].

Accurate theoretical modeling of strong many-body electron-electron interactions in the valence d shells of transition metal atoms is challenging for the approximate density functionals [7,14,15]. Local density approximation [16] (LDA), generalized gradient approximation [17] (GGA), and SCAN predict ZB ground state for CoO [8]. Hubbard U and J corrections [18–20] are commonly used to model repulsive Coulomb interactions on the strongly correlated d electrons. LDA+U+J [21] and PBE+U+J [22] predict the correct energetic ordering between CoO polymorphs. However, PBE+U [22] and SCAN+U [8] still predict an incorrect ZB ground state for CoO. In Table I, we show that our DFT and DFT+U calculations also agree with these findings. U parameter can be determined self-consistently using linear response theory [23]. However, suitable U and J parameters are often chosen based on their agreement with the experimental results which compromise the *ab initio* character of such calculations. Various U parameters were used on CoO polymorphs ranging from 3.3 to 8 eV depending on the properties studied, such as magnetic moments, electronic band gaps, and magnetic transitions [9,21,22,24,25]. It is well known that local and semilocal density functionals can drastically underestimate the band gap, and more advanced methods typically increase the band gap to near below and at the experimental range [7]. Different experimental techniques yield RS-CoO as an insulator with a band gap of 2.5–6 eV [26–30]. It has been argued that an accurate measurement of the band gap of CoO is challenging due to d-d intraband transitions [27]. SIC-LDA predicts a band gap of 2.81 eV [31]. Green's function [32] (G_0W_0) method predicts a band gap of 2.47 eV [33] and 3.4 eV [34] demonstrating a strong dependence on the input orbitals. Therefore, it can be of great scientific interest to explore the ground- and excited state properties of CoO, using a many-body theoretical method which is more robust with respect to starting conditions, such as diffusion quantum Monte Carlo (DMC) [35,36].

In this paper, we investigate structural, ground-, and excited state properties of CoO polymorphs using DMC. DMC can explicitly account for the antisymmetry of the many-body wave function and electron correlation, without using any empirical parameters [35]. DMC is capable of near chemical accuracy for both ground and excited states [36–40], while achieving a scaling of $O(N^3)$ with constant statistical error bar [41,42]. Here, N is the number of electrons in the simulation. With recent advances in computational capabilities, DMC has already been applied to various properties in binary transition metal oxides such as FeO [39], NiO [43,44], MnO [12], TiO_2 [37,45,46], Ti_4O_7 [47], VO_2 [48,49], and ZnO [37,50,51]. While Co dimers and Co-containing

*saritask@ornl.gov
†reboredo@ornl.gov

TABLE I. Equilibrium volume (V_0, in Å^3/f.u.), bulk modulus (B_0, in GPa), cohesive energy (E_{coh}, in eV/f.u.) of rocksalt (RS) CoO, and total energies of the wurtzite (WZ) and zinc-blende (ZB) phases with respect to the RS phase ($\Delta E_{WZ/RS}$ and $\Delta E_{ZB/RS}$ respectively, in units of eV/f.u.).

	RS			WZ			ZB		
	V_0 (Å^3)	B_0 (GPa)	E_{coh} (eV/f.u.)	V_0 (Å^3)	B_0 (GPa)	$\Delta E_{WZ/RS}$ (eV/f.u.)	V_0 (Å^3)	B_0 (GPa)	$\Delta E_{ZB/RS}$ (eV/f.u.)
PBE	18.86	189	9.70	23.16	131	−0.188	22.70	127	−0.260
PBE+U	19.61	171	9.50	24.47	128	−0.037	24.18	128	−0.061
PBE+U+vdW[a]	19.12	183	9.92	24.30	136	−0.010	24.08	135	0.041
SCAN	18.94	204	10.47	23.22	152	−0.038	22.93	146	−0.091
SCAN+U	19.18	189	10.45	23.86	145	0.071	23.68	147	0.063
SCAN+U+vdW[b]	19.06	192	10.59	23.72	148	0.110	23.53	149	0.102
HSE	19.23	200	8.93	23.71	143	−0.030	23.96	146	−0.043
DMC	19.23(3)	179(12)	9.5(1)	23.58(7)	143(8)	0.28(5)[c]	23.67(6)	144(6)	0.37(5)
Experiment	19.25 [76]	180 [54]	9.45 [55,56]	23.71 [6]	N/A	0.27 [2],0.26 [4]	23.55 [77]	N/A	∼0.4(1) [1,2]

[a]TS vdW correction [83].
[b]rvv10 vdW correction [84].
[c]Semiempirical calculations.

molecular complexes have been studied previously, to our knowledge, DMC has not yet been applied to study bulk Co oxides [52,53].

II. METHODS

A. Diffusion Monte Carlo

Here, we only provide a brief overview of the diffusion Monte Carlo approach. Additional details can be found in Refs. [35,36,38]. Diffusion Monte Carlo estimates the ground-state energy of the many-body problem by simulating the evolution of the wave function in imaginary time, τ:

$$\frac{\partial}{\partial\tau}\Psi(\mathbf{R},\tau) = \left(-\frac{1}{2}\nabla^2 + V - E\right)\Psi(\mathbf{R},\tau). \quad (1)$$

Here ∇^2 and V are the kinetic and potential energy operators, $\Psi(\mathbf{R},\tau)$ is the wave function, and E is the ground-state energy offset. By adjusting the ground-state energy offset, higher energy states are exponentially damped in the equilibration phase of the DMC calculations. Once the steady state is reached, the ground state is projected out statistically.

To solve Eq. (1), an initial or trial wave function $\Psi_T(\mathbf{R},t)$ is provided, which is then projected through importance sampling [57]. The trial wave function is typically obtained as a product of Slater determinants from DFT calculations and variational Monte Carlo (VMC) optimized Jastrow factors:

$$\Psi(\mathbf{R},\tau) = D^{\uparrow}(\mathbf{R})D^{\downarrow}(\mathbf{R})e^{-(J_1+J_2+J_3)}. \quad (2)$$

Here $D^{\uparrow}$ and $D^{\downarrow}$ are the spin up and spin down Slater determinants obtained from DFT calculations in our work, while J_1, J_2, and J_3 terms refer to the one-body, two-body, and three-body Jastrow terms, respectively. VMC calculations can typically recover 60%–90% of the total valence correlation energy [58]. Therefore, they are mainly used to optimize the Jastrow parameters. DMC calculations are then used to recover the remaining correlation energy.

B. Computational details

Practical DMC calculations on realistic materials require several approximations. A detailed explanation of these approximations and test calculations are given in the Supplemental Material [59]. QMC calculations were performed using QMCPACK [60], while DFT-QMC calculation workflows were generated using Nexus [61] software suite. We used the locality approximation to reduce localization error in DMC calculations [62–64]. Model periodic-Coulomb (MPC) [65,66] interaction was used to eliminate spurious two-body interactions on the potential energy [65,66]. We have included up to three-body Jastrow [58] parameters to optimize the trial wave function, using variance and energy minimization [67] consecutively. Various sophisticated methods can be used to optimize the nodal surface of the trial wave function [68–71]. However, we generated single particle Slater determinants within the LDA+U [18,24] approach, using QUANTUM ESPRESSO [72] code. These DFT orbitals were then used as trial wave functions for the DMC calculations. Here, the U parameter was only used as a variational parameter in DMC to optimize the nodal surface of the trial wave function. For all three CoO phases, the minimum total energies were obtained at $U = 5$ eV. Charge densities optimized at different U values are cross-checked as the starting charge densities to ensure correct orbital ordering in each LDA+U calculation [73]. For Co and O atoms, we used hard LDA RRKJ pseudopotentials that had been generated using OPIUM [74] code and tested for use in QMC [75]. Here, we used a kinetic energy cutoff of 350 Ry. A time step of 0.01 Ha^{-1} and $3 \times 3 \times 3$ reciprocal twist were used in all DMC calculations. Finite size extrapolations were made using up to 64 atom simulation cells for the energy differences between the polymorphs (Fig. 1), whereas 32 atom cells were used for the equation of states calculations.

Experimental coordinates [6,76,77] were scaled isotropically to obtain energy versus volume curves. We used Murnaghan's equation of state [78] fits to obtain bulk moduli. For the excited state DMC calculations, we identified the conduction band (CBM) and valence band maxima (VBM)

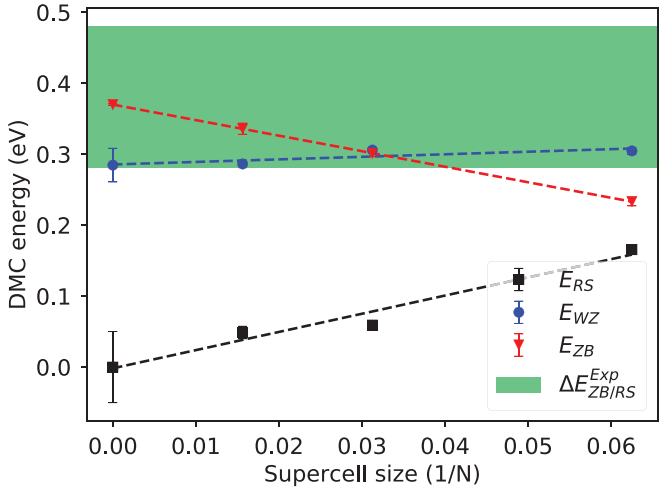

FIG. 1. DMC energies of rocksalt (RS), wurtzite (WZ), and zinc-blende (ZB) phases of CoO. Energies on the y axis are shifted by -161.43905 Ha, which is the DMC energy of the RS phase extrapolated at infinity. Extrapolations are performed using jackknife sampling. Experimental energy difference between the RS and ZB phases, $\Delta E_{RS/ZB}$, is shown with the green shaded area. If not shown, error bars on the DMC energies are smaller than the marker size.

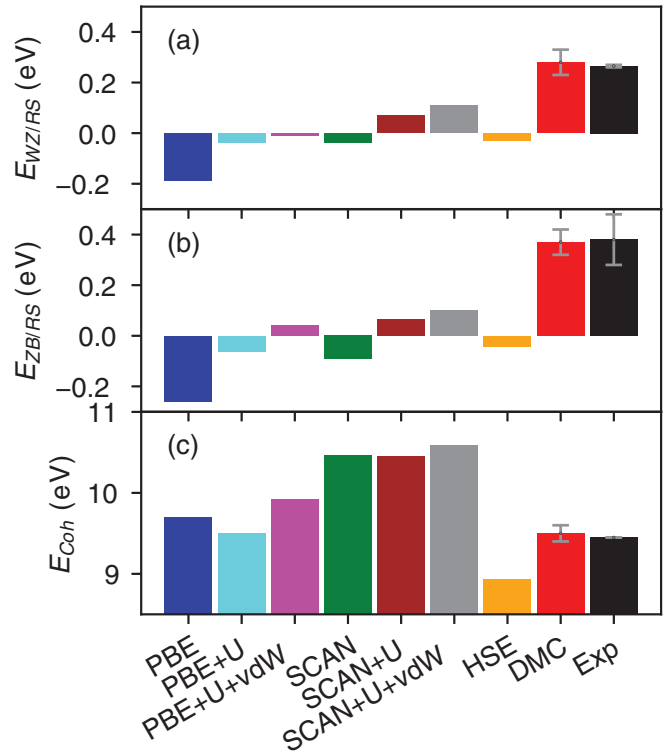

FIG. 2. Stability of the (a) WZ and (b) ZB phases compared to the RS phase. (c) Cohesive energy of the RS phase. Seven DFT functionals and DMC results are compared with respect to experiments. All values in y axes are given in eV.

using PBE+U. We calculated zero-point energies at the DFT-PBE level using PHONOPY [79]. For benchmark DFT and DFT+U calculations, we used the Vienna *ab initio* simulation package [80,81] (VASP) code. Projector-augmented wave pseudopotentials [82] were used to replace the core electrons and a kinetic energy cutoff is chosen as 520 eV. We used self-consistently determined $+U$ values of 3.4 and 2.9 eV for PBE+U and SCAN+U calculations [8]. Complementary vdW corrections [83,84] for the DFT+U functionals in this study were obtained from Ref. [8].

III. RESULTS

A. Ground-state energies and phase stability

Below the Néel temperature ($T_N = 287$ K) RS-CoO is a type-II antiferromagnet (AFM-II) [76,85–87]. Unlike RS-CoO, there is no experimental information regarding the magnetic configuration of WZ and ZB-CoO. DFT calculations shows that, for WZ and ZB, AFM-I and AFM-III magnetic configurations are the ground states with only 2–3 meV energy difference [22,88]. Therefore, in our DMC calculations, we used the AFM-I magnetic configuration for both WZ and ZB. Detailed illustrations of the crystal structures and the magnetic configurations are given in the Supplemental Material [59].

Finite size extrapolations of DMC ground state energies are shown for RS, WZ, and ZB phases in Fig. 1. In Fig. 1, the x axis represents the inverse number of atoms given in each simulation cell, while the y axis is the DMC energy per formula unit. Our results are summarized in Table I and energetic quantities are plotted in Figs. 2(a) and 2(b). DMC energy difference between ZB and RS CoO, $\Delta E_{ZB/RS}$, is 0.37(5) eV, which is in excellent agreement with the experimental value: $\Delta E^{Expt}_{ZB/RS} \approx 0.4 \pm 0.1$ eV (37 ± 10 kcal/mol) [1]. $\Delta E^{DMC}_{WZ/RS}$ is equal to 0.28(5) eV, which contains the semiempirical [2] and indirect estimates [4] of $\Delta E_{WZ/RS}$ with 0.26–0.27 eV within statistical errors. None of the standalone DFT approaches we investigated are successful at predicting the correct energy differences between the ZB and RS phases. Figure 2 shows that $+U$ correction on SCAN functional yields the qualitatively correct $\Delta E_{ZB/RS}$ and the results are slightly improved with the addition of the van der Waals (vdW) corrections. However, SCAN+U predicts WZ energetically more favorable than to ZB, which is incorrect with respect to experiments.

Table I and Fig. 2(c) show that the best agreement with the experimental cohesive energy of RS-CoO is obtained with PBE+U and DMC. PBE+U cohesive energy is 9.50 eV/f.u., while DMC cohesive energy is 9.5(1) eV/f.u. Experimental cohesive energy, 9.45 eV/f.u., is within the 1-σ error of the DMC cohesive energy. Significant overestimation of the cohesive energies, larger than 10 eV, with SCAN might be related to pseudopotential error in the gas phase calculation. Figure 2(c) shows that $+U$ corrections decrease the cohesive energy, while vdW corrections lead to an increase. When $+U$ or vdW corrections are applied on SCAN functional, similar but less dramatic changes are observed compared to PBE.

B. Structural properties

DFT functionals can typically yield reasonable bulk moduli due to the cancellation of errors between the isotropically scaled structures [89]. In addition to the numerical values in

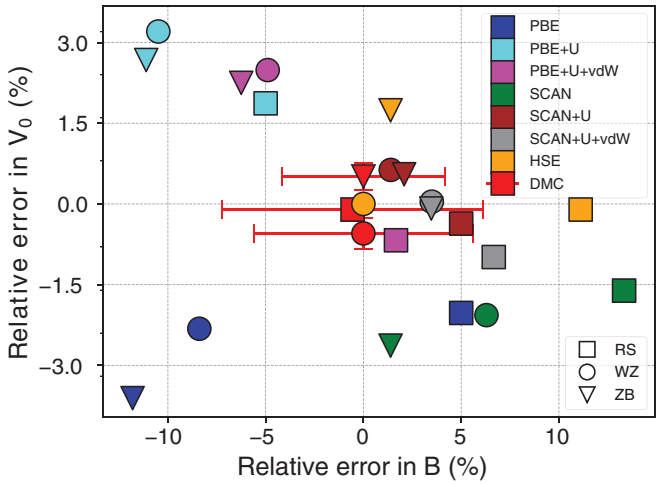

FIG. 3. Relative errors (in %) of V_0 versus B. Each DFT functional is given a color code, shown in the legend, while RS, WZ, and ZB results are shown using squares, circles, and triangles, respectively. DMC bulk moduli is used as the reference for WZ and ZB phases, while experiments in Table I are used for RS. Error bars on DMC results are smaller than marker size, when not visible.

Table I, relative errors in equilibrium volume V_0 and bulk moduli B are given in Fig. 3 for better visual representation. Energy versus volume curves for all phases can be found in the Supplemental Material [59]. In Fig. 3, each DFT functional is shown in different colors, while the RS phase is shown with squares; WZ and ZB phases are shown in circles and triangle, respectively. Experimental equilibrium volumes and bulk moduli are used as the reference whenever possible. Experimental bulk moduli of WZ and ZB phases are not available to our knowledge; therefore, DMC bulk moduli are used as the reference. In Fig. 3, SCAN+U, SCAN+U+vdW, and PBE+U+vdW bulk moduli are within or near the 1-σ uncertainties of the DMC bulk moduli for all phases. DMC bulk moduli are rather sensitive to the uncertainties in energy vs volume curves, but a comparison among DFT bulk moduli can also be useful. SCAN functional yields larger bulk moduli compared to PBE. In RS and WZ-CoO, $+U$ interactions decreases the bulk moduli, while bulk modulus of ZB-CoO is only slightly increased with $+U$ interactions. The bulk moduli are increased with vdW and $+U$ interactions. VdW interactions are more attractive in the short range and they increase the curvature of the energy versus volume curve. This effect is more pronounced in RS CoO, due to its larger coordination number and ionicity.

In Fig. 3, SCAN+U yields the most accurate equilibrium volumes compared to all DFT functionals investigated. General improvement of the standalone DFT functionals follows "Jacob's ladder": SCAN and SCAN+U perform better than PBE and PBE+U, respectively. While PBE and SCAN underestimate the equilibrium volume, PBE+U largely overestimates. It is well known that $+U$ interactions yield larger equilibrium volumes compared to standalone DFT functionals due to enhanced repulsive interactions between the electrons [90]. We find that vdW corrections yield smaller equilibrium volumes in both PBE and SCAN, due to the additional attractive interactions in the short range [38]. Except for RS-CoO, SCAN+U+vdW achieves perfect agreement with experimental equilibrium volumes. The DMC equilibrium volumes of all polymorphs are in good agreement with the experimental values, within the statistical error bars.

TABLE II. Excited state properties of RS CoO. Indirect and direct band gaps from DFT calculations correspond to the generalized Kohn-Sham eigenvalue differences from band-structure calculations. DMC_{QP} is the quasiparticle gap calculated using DMC. All quantities are given in eV.

	Indirect gap ($K \rightarrow \Gamma$)	Direct gap ($\Gamma \rightarrow \Gamma$)
PBE	0	
SCAN	0.94	1.50
PBE+U	2.22	2.61
SCAN+U	1.65	2.94
HSE [34]	3.2	4.0
HSE-G_0W_0 [34]	2.47 [33], 3.4	4.5
DMC	3.8(2)	5.2(2)
DMC_{QP}	3.9(2)	5.5(2)
Expt.	2.5(3) [26], 5.43 [27], 2.8 [28], 6 [30], 3.6(5) [91]	

C. Excited state properties

In Table II, we show DMC and DFT study of excited states in RS-CoO. For RS-CoO, photoemission studies find a gap of 2.5 ± 0.3 eV [26] and 6.0 eV [30], optical absorption yields a gap of 2.8 eV [28], and conductivity studies report a band gap of 3.6 ± 0.5 eV [91]. However, ellipsometry studies showed that these smaller band gaps can be intraband transitions within the d band and the direct band gap of the material is 5.43 eV [27]. Powell and Spicer [92] compared the optical absorption spectra of NiO and CoO, and show that their absorption spectrum is very similar in character. Since CoO absorption edge occurs at a higher energy than in NiO, the band gap of Co must be larger than the band gap of NiO [26,30]. In comparison, the band gap of NiO is well studied to be between 3.7 and 4.3 eV [27,29,92,93]. With this survey of experimental studies, we conclude that the band gap of CoO is controversial; however, the ellipsometry studies have been able to explain the lower energy transitions that are measured in other studies.

Our DMC results on the excited states of RS-CoO agree with several experimental and computational studies. DMC indirect quasiparticle gap is 3.9(2) eV, while the direct quasiparticle gap is 5.5(2) eV. Our DMC direct gap quasiparticle gap is in close agreement with the ellipsometry studies in Ref. [27]. We present the quasiparticle gap value here along with the DFT Kohn-Sham band gaps and DMC optical gaps in Table II. Our DMC indirect and direct optical band gap results are 3.8(2) and 5.3(2) eV, respectively. These results are in close agreement with the conductivity measurements [91] and GW calculations [33]. These results also imply an exciton binding energy of nearly 0.3(2) eV, which is within the statistical errors of zero.

IV. CONCLUSIONS

We studied the three known polymorphs of CoO using DMC. Although molecules and clusters involving Co have

been studied using DMC, our work was an attempt involving a bulk Co system. We showed that DMC is able to provide excellent agreement with the experimental data on the energy differences between the polymorphs and the bulk moduli. Our study shows the deficiencies of DFT methods in such properties of cobalt oxides, which can only be partially corrected using empirical interaction terms. We showed that none of the studied DFT functionals are able to provide correct energetic ordering between the three polymorphs of CoO. The success of DMC in these properties will facilitate more accurate theoretical results in other properties such as phase diagrams and magnetic transitions in cobaltite phases.

ACKNOWLEDGMENTS

The work was supported by the US Department of Energy, Office of Science, Basic Energy Sciences, Materials Sciences and Engineering Division. Computational resources were provided by the Oak Ridge Leadership Computing Facility at the Oak Ridge National Laboratory, supported by the Office of Science of the US Department of Energy under Contract No. DE-AC05-00OR22725.

[1] J. DiCarlo and A. Navrotsky, J. Am. Ceram. Soc. **76**, 2465 (1993).
[2] R. W. Grimes and K. P. D. Lagerlof, J. Am. Ceram. Soc. **74**, 270 (1991).
[3] A. Navrotsky and O. Kleppa, J. Inorg. Nucl. Chem. **29**, 2701 (1967).
[4] A. Navrotsky and A. Muan, J. Inorg. Nucl. Chem. **33**, 35 (1971).
[5] J. Dunitz and L. Orgel, J. Phys. Chem. Solids **3**, 318 (1957).
[6] A. S. Risbud, L. P. Snedeker, M. M. Elcombe, A. K. Cheetham, and R. Seshadri, Chem. Mater. **17**, 834 (2005).
[7] L. Wang, T. Maxisch, and G. Ceder, Phys. Rev. B **73**, 195107 (2006).
[8] H. Peng and J. P. Perdew, Phys. Rev. B **96**, 100101(R) (2017).
[9] D.-H. Seo, A. Urban, and G. Ceder, Phys. Rev. B **92**, 115118 (2015).
[10] J. Sun, R. C. Remsing, Y. Zhang, Z. Sun, A. Ruzsinszky, H. Peng, Z. Yang, A. Paul, U. Waghmare, X. Wu, M. L. Klein, and J. P. Perdew, Nat. Chem. **8**, 831 (2016).
[11] D. A. Kitchaev, H. Peng, Y. Liu, J. Sun, J. P. Perdew, and G. Ceder, Phys. Rev. B **93**, 045132 (2016).
[12] J. A. Schiller, L. K. Wagner, and E. Ertekin, Phys. Rev. B **92**, 235209 (2015).
[13] H. Peng and S. Lany, Phys. Rev. B **87**, 174113 (2013).
[14] E. Dagotto, Science **309**, 257 (2005).
[15] Y. Tokura and N. Nagaosa, Science **288**, 462 (2000).
[16] J. P. Perdew and A. Zunger, Phys. Rev. B **23**, 5048 (1981).
[17] J. P. Perdew, K. Burke, and M. Ernzerhof, Phys. Rev. Lett. **77**, 3865 (1996).
[18] V. I. Anisimov, F. Aryasetiawan, and A. I. Lichtenstein, J. Phys.: Condens. Matter **9**, 767 (1997).
[19] S. L. Dudarev, G. A. Botton, S. Y. Savrasov, C. J. Humphreys, and A. P. Sutton, Phys. Rev. B **57**, 1505 (1998).
[20] A. Georges, G. Kotliar, W. Krauth, and M. Rozenberg, Rev. Mod. Phys. **68**, 13 (1996).
[21] R. Hanafin, T. Archer, and S. Sanvito, Phys. Rev. B **81**, 054441 (2010).
[22] H.-X. Deng, J. Li, S.-S. Li, J.-B. Xia, A. Walsh, and S.-H. Wei, Appl. Phys. Lett. **96**, 162508 (2010).
[23] M. Cococcioni and S. de Gironcoli, Phys. Rev. B **71**, 035105 (2005).
[24] V. I. Anisimov, J. Zaanen, and O. K. Andersen, Phys. Rev. B **44**, 943 (1991).
[25] W. E. Pickett, S. C. Erwin, and E. C. Ethridge, Phys. Rev. B **58**, 1201 (1998).
[26] J. van Elp, J. L. Wieland, H. Eskes, P. Kuiper, G. A. Sawatzky, F. M. F. de Groot, and T. S. Turner, Phys. Rev. B **44**, 6090 (1991).
[27] T. Dong, H. Suk, and H. Hosun, J. Korean Phys. Soc. **50**, 632 (2007).
[28] G. W. Pratt and R. Coelho, Phys. Rev. **116**, 281 (1959).
[29] Y. Ksendzov and I. Drabkin, Fizika Tverdogo Tela (Sankt-Peterburg) **7**, 1884 (1965).
[30] Z.-X. Shen, J. W. Allen, P. A. P. Lindberg, D. S. Dessau, B. O. Wells, A. Borg, W. Ellis, J. S. Kang, S.-J. Oh, I. Lindau, and W. E. Spicer, Phys. Rev. B **42**, 1817 (1990).
[31] A. Svane and O. Gunnarsson, Phys. Rev. B **37**, 9919(R) (1988).
[32] L. Hedin, Phys. Rev. **139**, A796 (1965).
[33] H. Jiang, R. I. Gomez-Abal, P. Rinke, and M. Scheffler, Phys. Rev. B **82**, 045108 (2010).
[34] C. Rödl, F. Fuchs, J. Furthmüller, and F. Bechstedt, Phys. Rev. B **79**, 235114 (2009).
[35] W. Foulkes, L. Mitas, R. Needs, and G. Rajagopal, Rev. Mod. Phys. **73**, 33 (2001).
[36] R. J. Needs, M. D. Towler, N. D. Drummond, and P. López Ríos, J. Phys.: Condensed Matter **22**, 023201 (2010).
[37] K. Saritas, T. Mueller, L. Wagner, and J. C. Grossman, J. Chem. Theory Comput. **13**, 1943 (2017).
[38] L. Shulenburger and T. R. Mattsson, Phys. Rev. B **88**, 245117 (2013).
[39] J. Kolorenc, S. Hu, and L. Mitas, Phys. Rev. B **82**, 115108 (2010).
[40] A. J. Williamson, R. Q. Hood, R. J. Needs, and G. Rajagopal, Phys. Rev. B **57**, 12140 (1998).
[41] A. J. Williamson, R. Q. Hood, and J. C. Grossman, Phys. Rev. Lett. **87**, 246406 (2001).
[42] D. Alfe and M. J. Gillan, J. Phys.: Condens. Matter **16**, L305 (2004).
[43] J. Yu, L. K. Wagner, and E. Ertekin, J. Chem. Phys. **143**, 224707 (2015).
[44] R. J. Needs and M. D. Towler, Int. J. Mod. Phys. B **17**, 5425 (2003).
[45] J. Trail, B. Monserrat, P. López Ríos, R. Maezono, and R. J. Needs, Phys. Rev. B **95**, 121108(R) (2017).
[46] Y. Luo, A. Benali, L. Shulenburger, J. T. Krogel, O. Heinonen, and P. R. C. Kent, New J. Phys. **18**, 113049 (2016).
[47] A. Benali, L. Shulenburger, J. T. Krogel, X. Zhong, P. R. C. Kent, and O. Heinonen, Phys. Chem. Chem. Phys. **18**, 18323 (2016).

[48] H. Zheng and L. K. Wagner, Phys. Rev. Lett. **114**, 176401 (2015).
[49] I. Kylänpää, J. Balachandran, P. Ganesh, O. Heinonen, P. R. C. Kent, and J. T. Krogel, Phys. Rev. Materials **1**, 065408 (2017).
[50] J. Yu, L. K. Wagner, and E. Ertekin, Phys. Rev. B **95**, 075209 (2017).
[51] J. A. Santana, J. T. Krogel, J. Kim, P. R. C. Kent, and F. A. Reboredo, J. Chem. Phys. **142**, 164705 (2015).
[52] K. Doblhoff-Dier, J. Meyer, P. E. Hoggan, G. J. Kroes, and L. K. Wagner, J. Chem. Theory Comput. **12**, 2583 (2016).
[53] Y. Virgus, W. Purwanto, H. Krakauer, and S. Zhang, Phys. Rev. B **86**, 241406(R) (2012).
[54] Q. Guo, H.-K. Mao, J. Hu, J. Shu, and R. J. Hemley, J. Phys.: Condens. Matter **14**, 11369 (2002).
[55] K. N. Jog, R. K. Singh, and S. P. Sanyal, Phys. Rev. B **31**, 6047 (1985).
[56] L. Glasser and D. A. Sheppard, Inorg. Chem. **55**, 7103 (2016).
[57] D. M. Ceperley and B. J. Alder, Phys. Rev. Lett. **45**, 566 (1980).
[58] N. D. Drummond, M. D. Towler, and R. J. Needs, Phys. Rev. B **70**, 235119 (2004).
[59] See Supplemental Material at http://link.aps.org/supplemental/10.1103/PhysRevB.98.155130 for details on equation of states and excited state calculations, approximations involving DMC calculations, details on optimizing LDA+U calculations, and crystal structures of all CoO polymorphs.
[60] J. Kim *et al.*, J. Phys.: Condens. Matter **30**, 195901 (2018).
[61] J. T. Krogel, Comput. Phys. Commun. **198**, 154 (2016).
[62] A. L. Dzubak, J. T. Krogel, and F. A. Reboredo, J. Chem. Phys. **147**, 024102 (2017).
[63] L. Mitáš, E. L. Shirley, and D. M. Ceperley, J. Chem. Phys. **95**, 3467 (1991).
[64] J. T. Krogel and P. R. C. Kent, J. Chem. Phys. **146**, 244101 (2017).
[65] N. D. Drummond, R. J. Needs, A. Sorouri, and W. M. C. Foulkes, Phys. Rev. B **78**, 125106 (2008).
[66] L. M. Fraser, W. M. C. Foulkes, G. Rajagopal, R. J. Needs, S. D. Kenny, and A. J. Williamson, Phys. Rev. B **53**, 1814 (1996).
[67] C. J. Umrigar and C. Filippi, Phys. Rev. Lett. **94**, 150201 (2005).
[68] Y. Kwon, D. M. Ceperley, and R. M. Martin, Phys. Rev. B **48**, 12037 (1993).
[69] Y. Kwon, D. M. Ceperley, and R. M. Martin, Phys. Rev. B **58**, 6800 (1998).
[70] P. Lopez Rios, A. Ma, N. D. Drummond, M. D. Towler, and R. J. Needs, Phys. Rev. E **74**, 066701 (2006).
[71] M. Bajdich, M. L. Tiago, R. Q. Hood, P. R. C. Kent, and F. A. Reboredo, Phys. Rev. Lett. **104**, 193001 (2010).
[72] P. Giannozzi *et al.*, J. Phys.: Condens. Matter **21**, 395502 (2009).
[73] B. Himmetoglu, R. M. Wentzcovitch, and M. Cococcioni, Phys. Rev. B **84**, 115108 (2011).
[74] Opium pseudopotential generator, http://opium.sourceforge.net.
[75] J. T. Krogel, J. A. Santana, and F. A. Reboredo, Phys. Rev. B **93**, 075143 (2016).
[76] W. Jauch, M. Reehuis, H. J. Bleif, F. Kubanek, and P. Pattison, Phys. Rev. B **64**, 052102 (2001).
[77] M. J. Redman and E. G. Steward, Nature (London) **193**, 867 (1962).
[78] F. D. Murnaghan, Proc. Natl. Acad. Sci. USA **30**, 244 (1944).
[79] A. Togo and I. Tanaka, Scr. Mater. **108**, 1 (2015).
[80] G. Kresse and J. Hafner, Phys. Rev. B **49**, 14251 (1994).
[81] G. Kresse and J. Furthmüller, Phys. Rev. B **54**, 11169 (1996).
[82] G. Kresse and D. Joubert, Phys. Rev. B **59**, 1758 (1999).
[83] A. Tkatchenko and M. Scheffler, Phys. Rev. Lett. **102**, 073005 (2009).
[84] M. Dion, H. Rydberg, E. Schröder, D. C. Langreth, and B. I. Lundqvist, Phys. Rev. Lett. **92**, 246401 (2004).
[85] D. Herrmann-Ronzaud, P. Burlet, and J. Rossat-Mignod, J. Phys. C: Solid State Phys. **11**, 2123 (1978).
[86] N. C. Tombs and H. P. Rooksby, Nature (London) **165**, 442 (1950).
[87] A. Schrön, C. Rödl, and F. Bechstedt, Phys. Rev. B **86**, 115134 (2012).
[88] M. J. Han, H.-S. Kim, D. G. Kim, and J. Yu, Phys. Rev. B **87**, 184432 (2013).
[89] K. Lejaeghere, V. Van Speybroeck, G. Van Oost, and S. Cottenier, Crit. Rev. Solid State Mater. Sci. **39**, 1 (2014).
[90] A. van de Walle and G. Ceder, Phys. Rev. B **59**, 14992 (1999).
[91] M. Gvishit and D. S. Tannhauser, J. Phys. Chem. Solids **33**, 893 (1972).
[92] R. J. Powell and W. E. Spicer, Phys. Rev. B **2**, 2182 (1970).
[93] G. A. Sawatzky and J. W. Allen, Phys. Rev. Lett. **53**, 2339 (1984).